Near-field infrared imaging with a microfabricated solid immersion lens

D. A. Fletcher,[a] K. B. Crozier, C. F. Quate, G. S. Kino, and K. E. Goodson
E. L. Ginzton Laboratory, Stanford University, Stanford, California 94305

D. Simanovskii and D. V. Palanker
Hansen Experimental Physics Laboratory, Stanford University, Stanford, California 94305

(Received 31 May 2000; accepted for publication 1 August 2000)

We report imaging in the infrared with a microfabricated solid immersion lens. The integrated 15-μm-diameter lens and cantilever are fabricated from single-crystal silicon and scanned in contact with a sample to obtain an image. We demonstrate a focused spot size of $\lambda/5$ and an effective numerical aperture of 2.5 with $\lambda=9.3$ μm light. The total power transmitted through the lens is a factor of 10^3 greater than through a metal aperture giving the same spatial resolution. Two 1.0 μm holes in a metal film separated by 3.0 μm are imaged with the solid immersion lens in transmission and shown to be resolved. © *2000 American Institute of Physics.* [S0003-6951(00)05239-6]

Circumventing the optical diffraction limit is important for imaging, data storage, photolithography, and spectroscopy. One technique is to pass light through an aperture placed close to a sample, where spatial resolution is determined by the diameter of the aperture. A major problem with this technique is the low optical throughput of apertures smaller than half a wavelength in diameter. Solid immersion microscopy[1] offers a method for achieving resolution below the diffraction limit in air with significantly higher optical throughput by focusing light through a high refractive-index solid immersion lens (SIL) held close to a sample. The minimum resolution of a focusing system is inversely proportional to numerical aperture (NA), where $\mathrm{NA}=n\sin\theta$, θ is the maximum angle of incidence, and n is the index of refraction at the focal point. Light with vacuum wavelength λ can be focused by an aberration-free lens to a spot whose full width at half maximum (FWHM) is $\lambda/(2\ \mathrm{NA})$ in the scalar diffraction limit, equivalent to Sparrow's criterion for spatial resolution. With solid immersion microscopy, improvements in NA and spatial resolution are proportional to the SIL refractive index.

Recent efforts have been directed at increasing the NA of solid immersion lenses for applications including imaging,[1–9] data storage,[10–12] and photolithography.[13] Mansfield and Kino[1] imaged 100 nm lines using 436 nm illumination and a hemispherical SIL, reaching an effective NA $=1.7$. Vollmer *et al.*[2] used a GaP hemispherical SIL to achieve low-temperature pump–probe spectroscopy with an effective NA$=1.2$, and Yoshita *et al.*[3,4] demonstrated low-temperature photoluminescence of quantum wells with an effective NA$=1.0$ using a hemispherical TaF-3 glass SIL. Terris *et al.*[10] used a Weierstrass optic, or supersphere, with the input beam focused to a point within the SIL a distance a/n from the center of the spherical SIL surface, where a is the radius of the sphere. They were able to write 317 nm bits in a magneto-optic material with $n=1.83$ at $\lambda=780$ nm, corresponding to an effective NA$=1.2$. Ghislain *et al.*[13] exposed 190 nm lines in photoresist using a hemispherical SIL with $n=2.2$ SIL at $\lambda=442$ nm. More recently, Wu *et al.*[7] imaged fluorescent spheres with a hemispherical GaP SIL, realizing an effective NA$=2.0$.

In this letter, we report imaging with a microfabricated solid immersion lens. We use a silicon lens 15 μm in diameter at a wavelength of 9.3 μm to demonstrate $\lambda/5$ resolution and an effective NA of 2.5. Use of the microfabricated SIL, whose diameter is comparable to the wavelength, gives a transmittance improvement of 10^3 over a metal aperture with equivalent resolution. The SIL is integrated onto a cantilever and scanned over a sample to collect an image. Si is useful for near- and mid-infrared wavelengths where it is transparent and has a high index ($n=3.4$).

The integrated SIL and cantilever shown in Fig. 1 are fabricated from the top Si of a silicon-on-insulator wafer.[14] Root-mean-squared (RMS) deviation of the lens radius from the average value is less than 5%, and RMS surface roughness is less than 5 nm measured from AFM scans. The focus of the lens is approximately 3 μm below the geometrical center of the lens, which is within 20% of the ideal for a

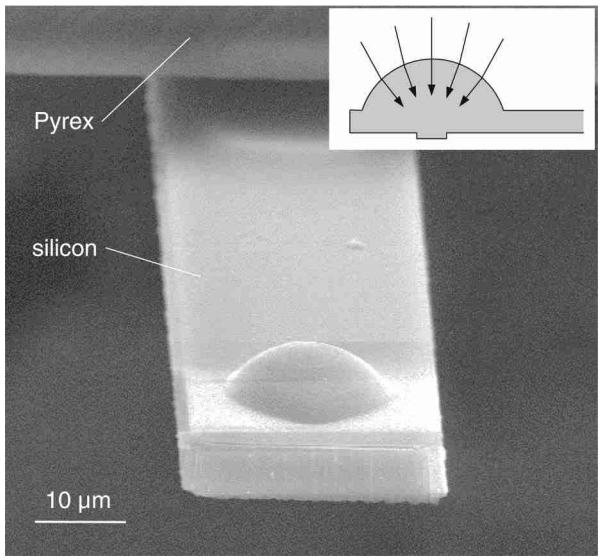

FIG. 1. Integrated solid immersion lens and cantilever fabricated from single-crystal Si and bonded to a Pyrex chip. The inset shows the lens and tip in profile and the ray paths of focused light.

[a]Electronic mail: dan.fletcher@stanford.edu

superspherical SIL. Small lenses benefit from a reduction in spherical aberration with diameter and can be refocused to compensate for errors in lens curvature and thickness. However, traditional methods for manufacturing cannot be used to make lenses smaller than ~1 mm in diameter. Microfabrication offers a technique for batch fabrication of lenses with diameters on the order of microns.

The microfabricated SIL and cantilever allow control of lens-sample separation through scanning. Even at wavelengths as long as $\lambda=9.3$ μm, a SIL made from Si must be placed closer than 200 nm to the sample surface for optimum transmittance and resolution. If topographical variations in the sample cause a greater separation between lens and sample, the exponential falloff and spreading of the focused fields in air cause a reduction in transmittance and resolution. It is difficult to maintain uniform contact with conventional SILs that are 1 mm in diameter due to sample topography and nonplanarity of the lens surface adjacent to the sample. Contact between the microfabricated SIL and sample is localized at a tip several microns in diameter, and the sample is scanned to form an image. Cantilevers with small lenses and large resonant frequencies can be scanned at high speeds across surfaces with high spatial frequency topography. For soft samples, the integrated SIL and cantilever can be held at a constant distance from the sample surface using force-feedback control. In this letter, results are reported for constant-contact scans on a hard sample for which feedback is not used.

We investigated spot size, transmittance, and imaging capabilities of the micromachined Si SIL with a CO_2 laser operating at $\lambda=9.3$ μm. A schematic of the experimental setup is shown in Fig. 2. The laser is focused by a reflecting objective (NA=0.45) onto the Si lens, which is fixed beneath the objective. A circular hole 1.0 μm in diameter in a metal film on a GaP substrate is scanned on an *XYZ* piezoelectric stage below the SIL. The opaque metal film consists of Cr (50 nm) on Au (50 nm). Light passing through the hole and collected by a second reflecting objective (NA=0.65) is measured with a liquid nitrogen-cooled HgCdTe detector. The hole is scanned in contact with the SIL to obtain minimum spatial resolution and maximum transmittance.

The FWHM of the fields below the Si SIL measured through the scanned 1.0 μm hole is 2.1 μm with $\lambda=9.3$ μm illumination, as shown in Fig. 3. The deconvoluted spot size of the SIL is estimated from a sum of squares to be 1.8 μm, corresponding to $\lambda/5$ resolution and an effective NA=2.5. This resolution represents the minimum theoretical spot size of light focused through Si with a 47 degree maximum angle of incidence (NA=0.74 in air). Though the SIL is illuminated with a maximum angle of incidence of 27 degrees (NA=0.45 in air), refraction at the lens surface increases the angle by a factor of approximately two and shifts the focus to the tip located below the geometrical center of the lens, similar to the superspherical SIL described by Terris *et al.*[10] Without the SIL, the FWHM of the focused beam is measured to be approximately 10.6 μm, close to the expected 10.3 μm spot size in air for NA=0.45 illumination. Use of the microfabricated SIL reduces the spot size by a factor of nearly six.

The total power transmitted through the microfabricated SIL with no sample in place is measured to be approximately 30% of the incident power. Reflection losses from the two Si surfaces account for a factor of 0.5, and the collection objective (NA=0.65) and total internal reflection at the tip reduce measured transmittance by a factor of approximately 0.4. The peak power collected through a 1.0 μm hole below the Si SIL is 25 times greater than that collected through the hole without the SIL. The increase in throughput results from greater power density above the hole due to focusing by the SIL and more efficient coupling of light through the hole due to the similarity in refractive index of Si ($n=3.4$) above and

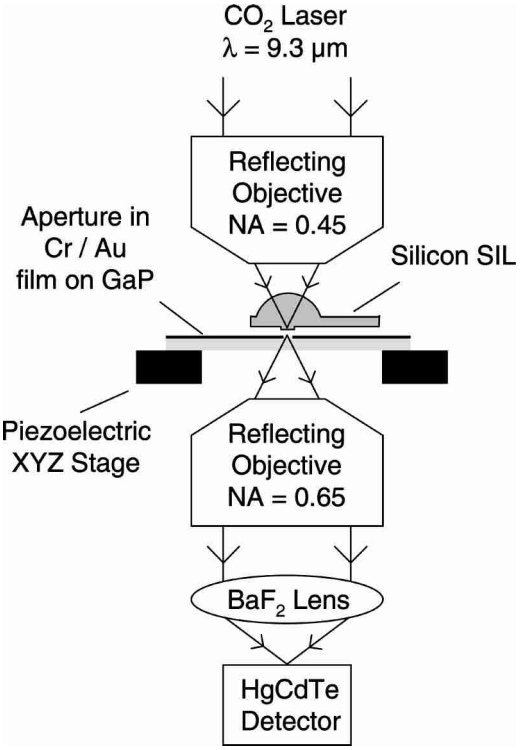

FIG. 2. Experimental setup used for imaging and measuring spot size with the Si SIL in transmission mode.

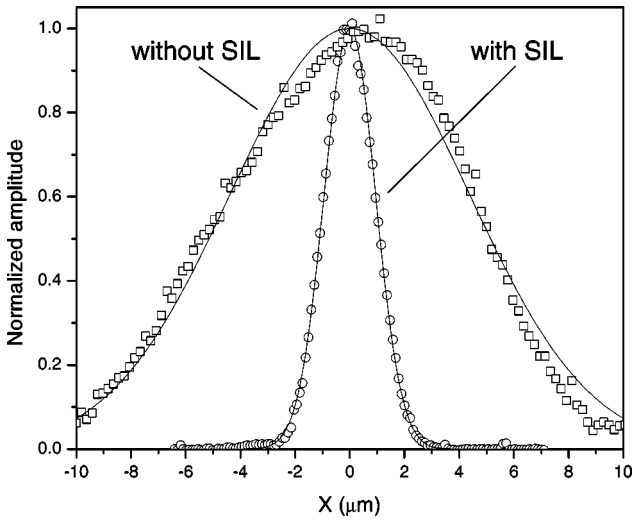

FIG. 3. Transmitted power through a 1.0-μm-diameter hole scanned at the focus of a CO_2 laser with (FWHM=2.1 μm) and without (FWHM=10.6 μm) the Si SIL. The data are fit to a Gaussian curve and normalized to a peak throughput of 1.0 in each case. The peak power measured with the SIL is 25 times greater than that measured without the SIL.

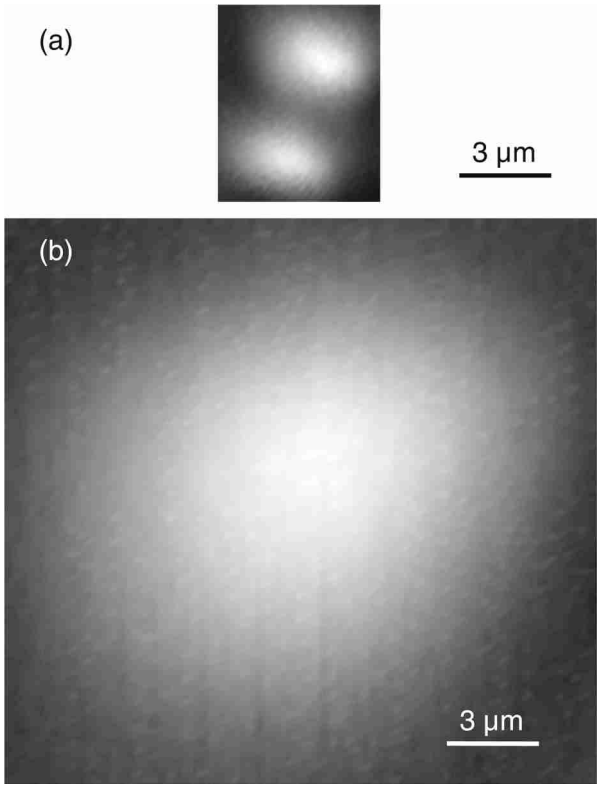

FIG. 4. Scanning infrared image taken (a) of two 1.0 μm holes separated by 3.0 μm with the Si SIL and (b) of focused $\lambda=9.3$ μm light without the Si SIL.

GaP ($n=3.0$) below the hole. However, the SIL does not require a metal hole to limit the lateral extent of the optical spot, and it does not suffer the losses in transmittance associated with aperture-based near-field probes.

The improvement in optical throughput of the SIL is significant when compared with the throughput of an aperture with equivalent spatial resolution. The Si SIL illuminated with a focused $\lambda=9.3$ μm beam can create a $\lambda/5$ spot with primarily reflection losses. By contrast, transmittance of the same focused beam through a 1.8-μm-diameter aperture with $\lambda/5$ resolution at $\lambda=9.3$ μm and with no SIL is measured to be $\sim 2\times 10^{-4}$. Though the SIL and the aperture achieve comparable spatial resolution, optical throughput of the SIL is a factor of 10^3 greater than that of the aperture.

The narrow focus created by the microfabricated SIL can be used to image subwavelength features in transmission. We are able to resolve two 1.0-μm-diameter holes in a Cr/Au film spaced by 3.0 μm with $\lambda=9.3$ μm light, as shown in Fig. 4(a). The focused spot without the SIL is shown in Fig. 4(b) for comparison. The infrared image is taken in the same way as the single hole scan, with light focused through the SIL and collected in transmission. The transmitted signal drops 70% between the two holes, suggesting that the holes could be more closely spaced and still resolved. This result compares well with an estimated 71% depth of modulation for two incoherent Gaussian spots with FWHM of 1.8 μm separated by 3.0 μm.

Several interesting applications exist for microfabricated SILs at infrared, visible, and ultraviolet wavelengths. The microfabricated Si SIL can be used to improve the spatial resolution and optical throughput of infrared thermometry, spectroscopy, and thermal processing of surfaces. Small lenses made of absorbing materials also transmit light more efficiently, enabling use of a wider range of wavelengths in materials normally considered opaque. The spatial resolution of microscopy and photolithography at visible and UV wavelengths may be improved by SILs fabricated from Si_3N_4 or other transparent materials.

In summary, we have demonstrated imaging with a microfabricated solid immersion lens. The SIL is fabricated from single-crystal Si and shown to focus $\lambda=9.3$ μm light to a $\lambda/5$ spot with an effective NA of 2.5. Power transmittance through the SIL is 10^3 times greater than that through a metal aperture giving equivalent spatial resolution. We also show that the Si SIL can resolve two 1.0 μm holes separated by 3.0 μm with $\lambda=9.3$ μm light.

This work was conducted with support from the Department of Energy, Semiconductor Research Corporation, Office of Naval Research, and the National Science Foundation. We made use of the Stanford Nanofabrication Facility, part of the National Nanofabrication Users Network funded by the NSF.

[1] S. M. Mansfield and G. S. Kino, Appl. Phys. Lett. **57**, 2615 (1990).
[2] M. Vollmer, H. Giessen, W. Stolz, W. W. Ruhle, L. Ghislain, and V. Elings, Appl. Phys. Lett. **74**, 1791 (1999).
[3] M. Yoshita, M. Baba, S. Koshiba, H. Sakaki, and H. Akiyama, Appl. Phys. Lett. **73**, 2965 (1998).
[4] M. Yoshita, T. Sasaki, M. Baba, and H. Akiyama, Appl. Phys. Lett. **73**, 635 (1998).
[5] C. D. Poweleit, A. Gunther, S. Goodnick, and J. Menendez, Appl. Phys. Lett. **73**, 2275 (1998).
[6] K. Koyama, M. Yoshita, M. Baba, T. Suemoto, and H. Akiyama, Appl. Phys. Lett. **75**, 1667 (1999).
[7] Q. Wu, G. D. Feke, R. D. Grober, and L. P. Ghislain, Appl. Phys. Lett. **75**, 4064 (1999).
[8] Q. Wu, R. D. Grober, D. Gammon, and D. S. Katzer, Phys. Rev. Lett. **83**, 2652 (1999).
[9] L. P. Ghislain and V. B. Elings, Appl. Phys. Lett. **72**, 2779 (1998).
[10] B. D. Terris, H. J. Mamin, D. Rugar, W. R. Studenmund, and G. S. Kino, Appl. Phys. Lett. **65**, 388 (1994).
[11] S. M. Mansfield, W. R. Studenmund, G. S. Kino, and K. Osato, Opt. Lett. **18**, 305 (1993).
[12] A. Chekanov, M. Birukawa, Y. Itoh, and T. Suzuki, Appl. Phys. Lett. **85**, 5324 (1999).
[13] L. P. Ghislain, V. B. Elings, K. B. Crozier, S. R. Manalis, S. C. Minne, K. Wilder, G. S. Kino, and C. F. Quate, Appl. Phys. Lett. **74**, 501 (1999).
[14] D. A. Fletcher, K. B. Crozier, G. S. Kino, C. F. Quate, and K. E. Goodson, Technical Digest of the Solid State Sensor and Actuator Workshop, Hilton Head, SC, 2000.